

## Spatiotemporal Characterization of Phagocytic NADPH Oxidase and Oxidative Destruction of Intraphagosomal Organisms *in Vivo* Using Autofluorescence Imaging and Raman Microspectroscopy

Wei-Tien Chang,<sup>†</sup> Yi-Cyun Yang,<sup>‡</sup> Hsueh-Han Lu,<sup>‡</sup> I-Lin Li,<sup>‡</sup> and Ian Liao<sup>\*‡</sup>

National Taiwan University College of Medicine and Hospital, Taipei, Taiwan, and Department of Applied Chemistry and Institute of Molecular Science, National Chiao Tung University, Hsinchu, Taiwan

Received October 9, 2009; E-mail: ianliao@mail.nctu.edu.tw

Professional phagocytes such as neutrophils and macrophages can engulf invading microbes into phagosomes and then produce antimicrobial oxidants and enzymes in the phagosome to destroy the ingested microbes.<sup>1</sup> Central to the oxidant-producing capability of a phagocyte is a transmembrane, multicomponent protein complex, a reduced nicotinamide adenine dinucleotide phosphate (NADPH) oxidase.<sup>2</sup> The necessity to assemble multiple components into a functioning NADPH oxidase enables regulated production of reactive-oxygen species (ROS) in phagocytes. When the phagocyte is in a resting state, the cytoplasmic subunits of the NADPH oxidase remain apart from flavocytochrome b<sub>558</sub> (cyt b<sub>558</sub>), the membrane-bound catalytic core of the enzyme; once activated, these components assemble on the membrane in preparation to generate superoxides. The produced superoxide and downstream ROS can avidly interact with vital biomolecules causing their irreversible destruction. Strict spatiotemporal orchestration of these molecular events is critical for proper operation of the phagocytic defense; recurrent life-threatening infections can occur for patients with defective NADPH oxidases,<sup>3</sup> but excessive production of ROS might damage cells or the extracellular matrix of the host inducing inflammatory disorder.<sup>4</sup>

Although phagocytic ROS has attracted much research, its intraphagosomal oxidative capacity has never been quantitatively measured; the question of which ROS plays a major role in the phagocytic oxidation also remains unanswered. Visualization of the NADPH oxidase was achieved mainly on stained and fixed cells;<sup>5</sup> few enable label-free characterization within a living cell. Here we demonstrate the use of autofluorescence imaging to track the spatiotemporal distribution of NADPH oxidases in living macrophages and Raman microspectroscopy to assess quantitatively the oxidative destruction of intraphagosomal microbes, employing no staining.

Our autofluorescence images show that there exist distinct bright spots in the cytoplasm of resting macrophages (Figure 1A) and that their number increases significantly after the macrophage is activated with lipopolysaccharides (Figure 1B). Quantitative analysis of images shows that the intensity increases over 6-fold after activation (Figure 1C). Significantly, the macrophages that are engulfing yeasts consistently and clearly exhibit a characteristic feature: these spots tend to gather in pseudopodia as the phagocyte is preparing to engulf yeasts (Figure 1D), and they become contiguous to and surround yeasts that have been completely internalized by a macrophage (Figure 1E). The latter feature is not seen for yeasts that remain extracellular and are not ingested.

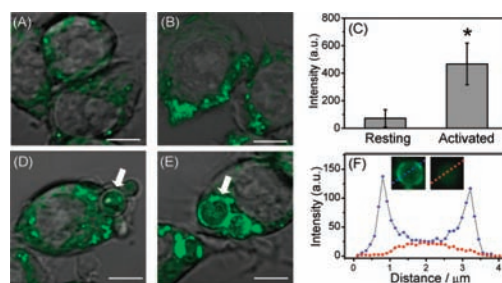


**Figure 1.** (A, B) Representative images of macrophages obtained before (A) and after (B) treatment with lipopolysaccharides (green: autofluorescence; gray: bright field). (C) Increase of fluorescence intensity after activation (\* $P < 0.001$ ,  $n = 17$ ). (D, E) Images showing macrophages engulfing yeasts (white arrows). (F) Line scans of a phagocytosed (blue) and an extracellular yeast (red). Scale bar: 5  $\mu\text{m}$ .

Comparison of the line scan obtained on a phagocytosed yeast with that on an extracellular yeast reveals clearly this distinction (Figure 1F).

Flavin adenine dinucleotide (FAD) is an endogenous fluorophore embedded in the catalytic core of NADPH oxidase (i.e., cyt b<sub>558</sub>) and serves to rely electron transport.<sup>2</sup> As NADPH oxidases are overexpressed in activated macrophages, it is conceivable to attribute to NADPH oxidase bound FAD the autofluorescence observed in macrophages. As a test of this assumption, we sought to identify the origin of the autofluorescence with measurements of the emission spectrum and fluorescence lifetime. Both the emission spectrum and the fluorescence lifetime recorded of macrophages agree satisfactorily with those of protein-bound FAD (Figure S1) and thus support our attribution. Despite there being other endofluorophores such as NADPH, our choice of excitation wavelength, 488 nm, and detection range, between 510 and 750 nm, both matching the spectral properties of FAD, facilitates a preferential detection of FAD over other endofluorophores.<sup>6</sup> To exclude mitochondrial FAD as the major source of the autofluorescence in macrophages, we performed similar measurements with treatment of antimycin A, a mitochondrial inhibitor that terminates the electron-transport chain in mitochondria, and prevents the formation of mitochondrial FAD.<sup>7</sup> The result shows that the characteristic feature seen in Figure 1E remains unaltered (Figure S2), thereby eliminating mitochondrial FAD as a major source of the autofluorescence observed in macrophages. Armed with these observations, we are content that the observed autofluorescence is contributed mainly from FAD bound in cyt b<sub>558</sub>, and the bright spots seen in the images of Figure 1 are attributed to NADPH oxidases.

We account for the above results as follows. The dim autofluorescence shown in Figure 1A indicates that the expression of the NADPH oxidase is halted for resting macrophages, whereas the

<sup>†</sup> National Taiwan University College of Medicine and Hospital.

<sup>‡</sup> National Chiao Tung University.

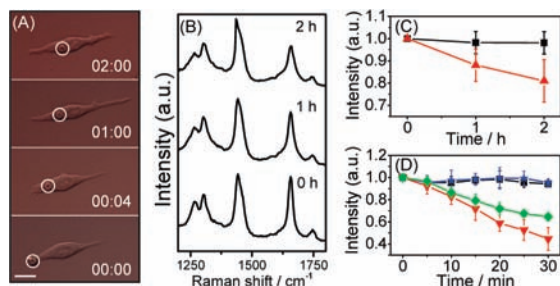


**Figure 2.** (A) Micrograph showing a macrophage engulfing a yeast (highlighted with a circle). (B) The corresponding kinetic Raman spectra measured for a phagocytosed yeast. (C) Time-varying intensities of the C=C Raman lines of single yeasts (black: control; red: phagocytosed yeasts;  $n = 3$ ). (D) Effect of various ROS on the C=C Raman lines of yeasts (black: control; blue: hydrogen peroxide; green: hypochlorous acid; red: hydroxyl radical). Scale bar: 20  $\mu\text{m}$ .

enhanced autofluorescence shown in Figure 1B and 1C indicates the overexpression of NADPH oxidases in activated macrophages. Moreover, Figure 1D and 1E reveal clearly that NADPH oxidases translocate to, and accumulate near, the phagosomes that entrap yeasts preparing to destroy the ingested microbes. A similar conclusion has been drawn with results obtained from Raman or immunofluorescence images of fixed and dead cells.<sup>5</sup> In comparison, our autofluorescence approach demonstrates spatiotemporal tracking of NADPH oxidases at various stages of phagocytosis in single, living macrophages, without stains.

As discussed above, the NADPH oxidase can generate intraphagosomal ROS to destroy phagocytosed microbes. In our previous work we demonstrated a label-free, molecular-level quantification of lipid peroxidation, a principal component of cellular oxidative injury, by probing the kinetic variation of the C=C Raman line associated with unsaturated lipids.<sup>8</sup> In the present work we extended this approach to explore the oxidative destruction of ingested microbes caused by phagocytic ROS and found that the C=C Raman line (at 1651  $\text{cm}^{-1}$ ) of the single phagocytosed yeasts declines progressively (Figure 2A and 2B). Specifically, 2 h after the onset of the phagocytosis, the intensity decreased by 19% ( $P = 0.00022$ ,  $n = 3$ ), whereas that of the control measurement on extracellular yeasts remained unaltered during the same period (Figure 2C). These results clearly show that, in detecting lipid peroxidation, the oxidative destruction of an intraphagosomal microbe caused by phagocytic ROS has been dynamically monitored. In contrast to the traditional assessment of phagocytosis that focuses mainly on the engulfing capability of phagocytes, our result demonstrates an unprecedented means to assess quantitatively the destructive capacity of phagocytic ROS at the level of single, living phagocytes without labeling, thus providing molecular-level insight into the functionality of phagocytosis.

Various ROS have been implicated in the phagocytic oxidation of ingested microbes. To elucidate their relative capacity to oxidize microbes, and to provide insight into which ROS plays a major role in the oxidant-dependent phagocytic defense, we performed Raman measurements on yeasts treated with various ROS. The results (Figure 2D) show that the C=C Raman line declines most markedly for yeasts treated with hydroxyl radical (55%,  $P = 2.8 \times 10^{-9}$ ;  $n = 11$ ); although milder, the oxidative effect of hypochlorous acid to the yeasts is also significant (35%,  $P = 2.2 \times 10^{-7}$ ;  $n = 7$ ), whereas, in contrast, hydrogen peroxide alone

causes no significant change of the C=C Raman line with time ( $P = 0.25$ ,  $n = 5$ ). These results indicate that hydroxyl radical and hypochlorous acids are likely to contribute to the oxidative destruction of the phagocytosed contents, whereas hydrogen peroxide, if not converted to hydroxyl radical through the Fenton reaction, or to hypochlorous acid through myeloperoxidase-mediated peroxidation, makes little contribution to the oxidative digestion of ingested microbes.

To demonstrate that combined autofluorescence imaging and Raman microspectroscopy can reveal mechanistic information that is otherwise difficult to obtain, we also characterized macrophages pretreated with apocynin, a catechol derivative that inhibits NADPH oxidases while not disturbing the phagocytic action of phagocytes.<sup>9</sup> We found that the C=C Raman line of yeasts that have been ingested in the apocynin pretreated macrophages remains intact (Figure S3), indicating that the oxidative capacity of apocynin pretreated macrophages is completely halted, whereas the autofluorescence images of these macrophages exhibit similar characteristic features seen in Figure 1E (Figure S4). The result not only provides compelling evidence that apocynin inhibits the NADPH-oxidase-facilitated oxidation of yeasts but also, for the first time, reveals that the inhibitory action of apocynin on NADPH oxidase does not affect the translocation of cyt b<sub>558</sub> to the phagosome.

By using autofluorescence imaging and Raman microspectroscopy, we have demonstrated label-free visualization of NADPH oxidases in living macrophages that are undergoing phagocytosis and quantitative assessment of phagocytic-ROS-caused oxidation occurring in intraphagosomal yeasts with no stains. In light of recent recognition of pathophysiological roles played by homologues of NADPH oxidases and ROS in cardiovascular and neurodegenerative diseases, we anticipate that extension of a similar approach to these systems might provide new mechanistic insight into relevant diseases such as atherosclerosis.

**Acknowledgment.** We thank Professors Y. P. Lee and Y. K. Li (NCTU) for their generous support and Drs. C. T. Yuan and C. Y. Chung for technical assistance. I.L. is funded by the National Science Council and the MOE-ATU program of Taiwan.

**Supporting Information Available:** Experimental details and supporting data. This material is available free of charge via the Internet at <http://pubs.acs.org>.

## References

- (a) Babior, B. M. *New Engl. J. Med.* **1978**, *298*, 659. (b) Burg, N. D.; Pillinger, M. H. *Clin. Immunol.* **2000**, *99*, 7. (c) Flannagan, R. S.; Cosio, G.; Grinstein, S. *Nat. Rev. Microbiol.* **2009**, *7*, 355.
- (a) Babior, B. M.; Kipnes, R. S. *Blood* **1977**, *50*, 517. (b) Bedard, K.; Krause, K. H. *Physiol. Rev.* **2007**, *87*, 245. (c) Nauseef, W. M. *Semin. Immunopathol.* **2008**, *30*, 195.
- Segal, A. W.; Cross, A. R.; Garcia, R. C.; Borregaard, N.; Valerius, N. H.; Soothill, J. F.; Jones, O. T. G. *New Engl. J. Med.* **1983**, *308*, 245.
- Rees, M. D.; Kennett, E. C.; Whitelock, J. M.; Davies, M. J. *Free Radical Biol. Med.* **2008**, *44*, 1973.
- (a) van Manen, H. J.; Uzunbajakava, N.; van Bruggen, R.; Roos, D.; Otto, C. *J. Am. Chem. Soc.* **2003**, *125*, 12112. (b) Casbon, A. J.; Allen, L. A. H.; Dunn, K. W.; Dinauer, M. C. *J. Immunol.* **2009**, *182*, 2325.
- Zipfel, W. R.; Williams, R. M.; Christie, R.; Nikitin, A. Y.; Hyman, B. T.; Webb, W. W. *Proc. Natl. Acad. Sci. U.S.A.* **2003**, *100*, 7075.
- Vonjagow, G.; Link, T. A. *Method. Enzymol.* **1986**, *126*, 253.
- Chang, W. T.; Lin, H. L.; Chen, H. C.; Wu, Y. M.; Chen, W. J.; Lee, Y. T.; Liau, I. *J. Raman Spectrosc.* **2009**, *40*, 1194.
- (a) Simons, J. M.; Hart, B. A.; Ip Vai Ching, T. R. A. M.; Van Dijk, H.; Labadie, R. P. *Free Radical Biol. Med.* **1990**, *8*, 251. (b) Stolk, J.; Hiltermann, T. J. N.; Dijkman, J. H.; Verhoeven, A. J. *Am. J. Resp. Cell Mol.* **1994**, *11*, 95.

JA9086038